Cement and Concrete Research 40 (2010) 109–118

Contents lists available at ScienceDirect

Cement and Concrete Research

journal homepage: http://ees.elsevier.com/CEMCON/default.asp

Comprehensive modeling of chloride ion and water ingress into concrete considering thermal and carbonation state for real climate

David Conciatori [a,*,1], Francine Laferrière [b], Eugen Brühwiler [a]

[a] EPFL – Laboratory of Maintenance and Safety of Structures, Swiss Federal Institute of Technology (EPFL), Lausanne, Switzerland
[b] EPFL – Applied Computing and Mechanics Laboratory, Swiss Federal Institute of Technology (EPFL), Lausanne, Switzerland

ARTICLE INFO

Article history:
Received 29 January 2009
Accepted 13 August 2009

Keywords:
Adsorption (C)
Carbonation (C)
Diffusion (C)
Chloride (D)
Thermal analysis (B)
Finite element analysis (C)

ABSTRACT

This article presents a comprehensive modeling of temperature, carbonation, water and chloride ions transport in cover concrete using the transport model "TransChlor". The TransChlor transport model employs weather data and chloride ion concentrations present on the concrete surface to predict the temporal and spatial evolution of the presence of chloride ion concentrations in the cover concrete pores. The main features of the TransChlor model are presented and validated.
The TransChlor model has been calibrated using experimental data on liquid water movement in concrete of different permeabilities under realistic microclimatic conditions. Chloride ion transport is validated by means of experimental results obtained from a newly developed chloride ion optical fiber based sensor.

1. Introduction

The initiation period of chloride induced steel reinforcement corrosion in reinforced concrete is the time it takes for chloride ions to penetrate from the concrete surface and migrate into the cover concrete until sufficient chloride ion concentration is present at the steel reinforcement to initiate steel corrosion. This initiation period is characterized by chemical conversions and material interactions between the various transport modes and ionic movements.

Microscopic and macroscopic models are often used to model the movement of chloride ions. Microscopic models describe chloride ion movements in concrete [29,31,51,54] and Schmidt-Döhl [50]. Macroscopic models consider the chemical conversions and the thermal, hydrous and chloride ion variations by simulating overall chemical effects on transport. Macroscopic models have been proposed by [7,19,27,32,44,45,53]. Although microscopic models simulate phase changes more precisely and consider changes of porosity, they often require extensive testing to calibrate model parameters.

This paper details the modeling of chloride ion ingress into concrete by respectively 1) an analytical investigation and 2) predictions and experimental results. The first part defines all equations and their parameters employed in the "TransChlor" model and explains and compares with physical observations. In the second part, the model is validated with own experimental results and results from the literature. These findings demonstrate that the "TransChlor" model reliably predicts chloride transport in reinforced concrete structural elements in contact with de-icing salts.

2. Research significance

To our knowledge, no prediction model of chloride ion ingress in cover concrete under real reconstituted microclimatic conditions currently exists [10,11]. TransChlor models chloride ion movement via capillary suction and pulled by liquid water. The liquid water transport model is based on experimental results at low temperature (−20 °C to 10 °C). The TransChlor model validation shows the potential of using a new fiber optic measuring device that permits to reliably record the ingress of chloride ions into the cover concrete. Precise modeling of chloride ion ingress into concrete is significant to predict durability of reinforced concrete structural elements.

3. Analytical investigation

The objective of the TransChlor model is to predict the initiation of reinforcing steel corrosion considering the actual reconstituted climatic and environmental actions applied on reinforced concrete structural elements. In addition to considering chloride ion diffusion in water, the model simulates aqueous chloride ion. Thus, this novel model complements the water vapor diffusion in the concrete with capillary suction of liquid water originating from precipitations.

* Corresponding author. Ecole Polytechnique de Montréal, David Conciatori, Département des génies civil, géologique et des mines, CP 6079, Station Centre-Ville, Montréal, (QC), Canada H3C 3A7. Tel.: +1 (514) 340 4711x3717.
E-mail address: david.conciatori@a3.epfl.ch (D. Conciatori).
[1] Current address: Polytechnic school of Montreal, Structural Research Group (GRS), Montreal, Canada.

0008-8846/$ – see front matter.
doi:10.1016/j.cemconres.2009.08.007

Before discussing the analytical investigation, general numerical arrangements will be presented. The time step chosen in the numerical simulations is set to 1 h. This time step is sufficient to precisely simulate temperature profiles, precipitations and water contact with the concrete surface. This time step also takes well into account alternate precipitation and drying periods which are a significant source of chloride ion movement in cover concrete. If the time step is increased to several hours, the precipitation periods will be accentuated, leading to an overestimation of ionic transport. This time step can be decreased if the variation of boundary conditions is important. This reduction prevents divergence of the numerical solution and consequently boundary conditions are interpolated linearly over this time interval.

The TransChlor transport model takes into account by a numerical approach the various transport modes (thermal and vapor transfer, liquid water transport with and without chloride ions, capillary suction, chloride ion diffusion in water, carbon dioxide diffusion in concrete).

The TransChlor model departs from structural modeling by segmenting the structure into distinct components in terms of functional role and corrosion vulnerability (i.e., cover concrete permeability, degree of exposure to corrosive agents, local defects, etc.). The model in particular distinguishes the structural elements exposed to water vapor and liquid water.

3.1. General equations

The chloride ion movement in the concrete is characterized by two transport modes: 1) aqueous chloride ion diffusion, and 2) aqueous chloride ion convection. The second transport mode is rather fast. It is even faster, when liquid water adsorption is due to capillarity and the structural element is under severe exposure conditions.

The transport model considers primarily two chemical reactions: 1) carbonation and 2) adsorption of chloride ions by the cement paste, the latter being a reversible transformation. The diffusion movements are the transfer of molecules or ions in the interstitial fluid from high to low concentrations. Diffusion is modeled with a simplified form of Fick's diffusion law. The liquid water movement by capillary suction is induced by the surface tension acting in the capillary pores. The liquid water movement is thus modeled using the kinetics equations. This equation is then transformed into chloride ion movement by a particular algorithm (simulating the convection of chloride ions by water).

The general formulation (1) considers all transport modes: thermal diffusion, carbonation, hydrous transport and chloride ion transport. The first term of the formulation (1) is modeled according to Fick's law, while the second term is a model for capillary suction Eq. (1). The parameter z is only used for the carbonation reaction Eq. (2).

$$\frac{\partial}{\partial t}\begin{Bmatrix} T \\ [CO_2] \\ H \\ C(B,T) \end{Bmatrix} = \operatorname{div}\left(A \cdot \begin{Bmatrix} \overrightarrow{\operatorname{grad}(T)} \\ \overrightarrow{\operatorname{grad}[CO_2]} \\ \overrightarrow{\operatorname{grad}(H)} \\ \overrightarrow{\operatorname{grad}(C(B,T))} \end{Bmatrix} \right) - E \cdot \begin{Bmatrix} \overrightarrow{\operatorname{grad}(T)} \\ \overrightarrow{\operatorname{grad}[CO_2]} \\ \overrightarrow{\operatorname{grad}(H)} \\ \overrightarrow{\operatorname{grad}(C(B,T))} \end{Bmatrix} - \begin{Bmatrix} 0 \\ z \\ 0 \\ 0 \end{Bmatrix} \tag{1}$$

$$z = -(\varepsilon_{ini} \cdot f_w \cdot r_{CH} + 3 \cdot r_{CSH} + 3 \cdot r_{C3S} + 2 \cdot r_{C2S}) \tag{2}$$

t time [s],
T temperature [°C],
$[CO_2]$ carbon dioxide molar concentration [mol/m^3 air],
H relative humidity in the concrete pores [−],
C total chloride ion concentration with respect to the concrete volume [kg/m^3],
B carbonation extent constant,
A matrix composed of the various diffusion and other coefficients,
E matrix composed of the convection and other coefficients,
z a carbonation parameter,
ε_{ini} initial porosity prior to hydration and carbonation [−],
fw ratio of pore and film water volume to the pore volume [−],
r_{CH} carbon dioxide reaction rate with portlandite [mol/s m^3 concrete],
r_{CSH} mean tricalcium and dicalcium silicate forming calcium silicate hydrates [mol/s.m^3 concrete],
r_{C3S} tricalcium silicate reaction rate [mol/s m^3 concrete],
r_{C2S} dicalcium silicate reaction rate [mol/s m^3 concrete].

The matrix A contains the Fick's diffusion law coefficients for thermal, carbon dioxide, vapor and chloride ion diffusion and the interaction between vapor and chloride ion diffusion Eq. (3).

$$A = \begin{bmatrix} \frac{\lambda_T(T,f)}{c_T(w)} & 0 & 0 & 0 \\ 0 & \frac{D_B(\varepsilon, H_{ext})}{\varepsilon \cdot (1-f)} & 0 & 0 \\ 0 & 0 & D_h(T,H) & 0 \\ 0 & 0 & R_{Cl} \cdot c_f(B) \cdot D_h(T) & D_{Cl} \end{bmatrix} \tag{3}$$

λ_T concrete thermal conductivity [W/(m K)],
f water content with respect to the water density [−],
c_T unit concrete heat-storage capacity [kJ/(m^3 K)],
w concrete water content per cubic meter of concrete [kg/m^3],
D_B carbon dioxide diffusion coefficient in concrete [mm^2/s],
ε pore volume with respect to the total concrete volume [−],
H_{ext} average atmospheric relative humidity between the concrete fabrication and current simulation time [−],
D_h water vapor diffusion coefficient [mm^2/s],
R_{Cl} delay coefficient,
c_f free chloride ion concentration in the concrete interstices with respect to the solution volume [kg/m^3],
D_{Cl} free chloride ion diffusion coefficient [mm^2/s].

The matrix E represents the material movement equations, the liquid water movement and the suction of chloride ions by liquid water Eq. (4).

$$E = \begin{bmatrix} 0 & 0 & 0 & 0 \\ 0 & 0 & 0 & 0 \\ 0 & 0 & D_{cap} & 0 \\ 0 & 0 & R_{Cl} \cdot c_f(B) \cdot D_{cap} & 0 \end{bmatrix} \tag{4}$$

D_{cap} capillarity coefficient [mm/s],

The resolution of the differential equations models space with a finite element method and time with a finite difference method. The simulations developed with the TransChlor model are one dimensional as in [44].

3.2. Thermal diffusion process

The rapid thermal transfer velocity facilitates the dissociation of thermal transfer from all other transport modes. Furthermore, the thermal inertia and the amount of water are considered. The heat-storage capacity of each concrete component, i.e., aggregates, cement

and water, is considered. The water consumption during cement hydration Eq. (5) is also taken into account following [18]. This leads to the following formulation:

$$c_T(w) = G \cdot c_S + C \cdot c_C + w_i \cdot c_w - 0.2 \cdot CP \cdot \alpha \cdot c_w \tag{5}$$

G mass quantity of aggregates in the concrete volume [kg/m^3],
c_S heat-storage capacity of aggregates [kJ/(kg K)],
C mass quantity of cement in the concrete volume [kg/m^3],
c_c heat-storage capacity of Portland cement [kJ/(kg K)],
i position index in the concrete,
c_w heat-storage capacity of water [kJ/(kg K)],
α degree of concrete hydration [−].

The heat-storage capacity of water is very important compared to the aggregates and the cement (Table 1). The water amount varies very quickly in the cover concrete which justifies a more precise modeling of the water transport in the cover concrete.

Thermal conductivity takes into account an internal thermal inertia due to the water temperature. Thus thermal conductivity depends on the concrete water content and temperature. The model is valid for temperatures higher than zero and up to 80 °C Eqs. (6) and (7). Both equations are developed by continuous polynomial interpolation. A Lagrange interpolation using the results from [18] yield the numbers presented below.

$$\begin{Bmatrix} a_1 \\ a_2 \\ a_3 \\ a_4 \\ a_5 \end{Bmatrix} = \begin{bmatrix} 1.899 & 3.368\cdot10^{-3} & -1.775\cdot10^{-4} & 3.195\cdot10^{-6} & -1.866\cdot10^{-3} \\ 1.502\cdot10^{-2} & -1.085\cdot10^{-3} & -4.893\cdot10^{-6} & 3.132\cdot10^{-7} & -2.668\cdot10^{-9} \\ -1.995\cdot10^{-3} & 7.17\cdot10^{-3} & -2.662\cdot10^{-4} & 3.634\cdot10^{-6} & -1.745\cdot10^{-8} \\ 9.336\cdot10^{-4} & -8.338\cdot10^{-4} & 3.1\cdot10^{-5} & -4.183\cdot10^{-7} & 1.978\cdot10^{-9} \\ -3.617\cdot10^{-5} & 2.26\cdot10^{-5} & -8.087\cdot10^{-7} & 1.046\cdot10^{-8} & -4.725\cdot10^{-11} \end{bmatrix} \times \begin{Bmatrix} T_i^0 \\ T_i^1 \\ T_i^2 \\ T_i^3 \\ T_i^4 \end{Bmatrix} \tag{6}$$

$$\lambda_T(T_i, f_i) = \sum_{j=1}^{5} a_j(T_i) \cdot f_i^{j-1} \tag{7}$$

a_j intermediate parameter for calculating thermal conductivity,
i position index in the concrete,
j parameters index.

The TransChlor model reference temperature is maintained at 0 °C. When the temperature is below 0 °C, the water content does not influence the cover concrete thermal transfer velocity [8]. Thus the isothermal curve at 0 °C corresponds to the minimal concrete values.

3.3. Carbonation

The carbonation model proposed in Eq. (1) considers that the carbonation depth is linear with the root of time. There are more complex models in literature (such as [14,19,47]), but none of these models have been validated experimentally. In addition, the TransChlor model shows little correlation between carbonation and the chloride movement in concrete. This simplified model is justified by the fact that carbonation influences the cement capacity to capture the chloride ions. The carbonation velocity varies with the ambient moisture conditions and exposure (urban, countryside or industrial environment, Table 2). The carbonation is considered in evaluating free and bound chloride ion concentration in the concrete. The temperature is also taken into account, but indirectly in the liquid water and vapor transport models.

The p_H profile in the cover concrete Eq. (8), used in the TransChlor model, takes into account the concrete zones not carbonated with a p_H value of 12.6 [40], concrete zones completely carbonated with a p_H value of 8.7 [40] and a linear transition zone for the partially carbonated zone. This transition zone ends where the concrete is regarded as carbonated defined by [16] (i.e. p_H value reaches 10.8). This interface corresponds to the carbonation depth obtained by the TransChlor model [36].

$$p_H = 12.6 \cdot \left[\frac{6.5}{12.6} + \frac{1 - 6.5/12.6}{1 + \left(\frac{1-(x - x_c + 2.88)/4}{1 - d_c} \right)^4} \right] \tag{8}$$

p_H transition zone p_H,
x depth of the cover concrete [mm],
x_c carbonation depth in the cover concrete [mm],
d_c model parameter equal 0.5 [−].

The mathematical model suggested by [6,14,41] following [36] considers:

- carbon dioxide diffusion in porous concrete,
- dissolution of carbon dioxide in the interstitial liquid phase,
- dissolution of portlandite,
- diffusion of aqueous carbon dioxide,
- reaction of concrete with dissolved carbon dioxide,
- carbon dioxide reaction on hydrated silicates and the unhydrated compounds including tricalcium and dicalcium silicates,
- reduction of pore volume due to carbonation,
- and water condensation on the pore walls produced during the carbonation.

The general carbon dioxide transport equation account for the filling rate of pores with water, the carbon dioxide dissolution in water, the portlandite formation by tricalcium and dicalcium silicate consumption [37].

Solving for the carbonation depth leads to Eq. (9), starting from the carbon dioxide transport Eq. (1). More details on the assumptions and simplifications in the present formulation are given in [8,38].

$$x_c = \frac{1}{16.75} \cdot \frac{\rho_c}{\rho_w} \cdot \frac{W/C - 0.3}{1 + (\rho_c/\rho_w) \cdot (W/C)} \cdot (1 - H_{ext}) \times \sqrt{\left(1 + \frac{\rho_c}{\rho_w} \cdot \frac{W}{C} + \frac{\rho_c}{\rho_G} \cdot \frac{G}{C}\right) \cdot y_{CO_2} \cdot t} \tag{9}$$

Table 1
Heat-storage capacity of concrete components [23].

Component	Heat-storage capacity [kJ/(kg K)]
c_S aggregates	
siliceous	0.73
limestone	0.84
lime + limestone	0.89
c_w	4.2
c_{CP}	0.84

Table 2
Carbon dioxide concentration in different environments [47].

Environment	Carbon dioxide concentration [vol.%]
Land	0.015
Town centre	0.036
Industrial area	0.045

W amount of mixing water with respect to concrete volume [kg/m^3],
ρ_C cement density [kg/m^3],
ρ_G aggregate density [kg/m^3],
ρ_w water density [kg/m^3],
y_{CO_2} carbon dioxide concentration in the air [−].

3.4. Hydrous transport of water vapor

Both transport modes of water vapor and liquid water capillary suction are separated in the TransChlor model following [1,20,44,48]. The TransChlor model uses Fick's law for the water vapor transport as given in [2,3]. This law simulates the diffusion of water vapor. The diffusion coefficient according to Eq. (10) utilizes temperature as determined by the Arrhenius' law [46] and the relative humidity present in the concrete pores [2]:

$$D_h(T,H) = D_{T_0} \cdot \left[\alpha_0 + \frac{1-\alpha_0}{1+\left(\frac{1-H}{1-H_c}\right)^n}\right] \cdot e^{\frac{Q}{R}\left(\frac{1}{T_0}-\frac{1}{T}\right)} \quad (10)$$

with:

D_{T_0} steady state diffusion coefficient at constant temperature [mm^2/s],
a_0, H_c, n Bazant's model coefficients,
Q Arrhenius' model activation energy [mol/J],
R gas constant (8.314510) [J/mol °C],
T_0 basic concrete temperature to determine Q and DT$_0$ [°C],
T concrete temperature [°C].

The steady state diffusion coefficient at constant temperature (Table 3) is obtained from tests on equivalent concretes as documented in the literature [11,15,17]. The same test results are also used in the transport models developed by [20,25,44].

The adsorption curve is modeled with the BET model which uses data obtained from hardened cement paste tests [57]. The TransChlor model transforms the BET model by adapting it for concretes following Eq. (11):

$$w_c(H) = \frac{C_{BET} \cdot k \cdot V_m \cdot H}{[1-(k \cdot H)] \cdot [1 + (C_{BET} - 1) \cdot k \cdot H]} \quad (11)$$

with:

C_{BET} water vapour adsorption parameter of the BET model,
k BET model parameter,
V_m mono-layer storage capacity,
w_c water content in the cement paste [g/g].

The parameter C_{BET} considers the total water vapour adsorption, the water vapour latent adsorption and the temperature, Eq. (12) [57]:

$$C_{BET} = e^{\frac{E_1 - E_L}{R \cdot T}} = e^{\frac{855}{T}} \quad (12)$$

with:

E_1 total water vapor adsorption [J/mol],
E_L latent water vapor adsorption [J/mol].

Table 3
Water vapor diffusion coefficient [44].

Concrete permeability	Diffusion coefficient D_{T_0} [10^{-6} mm^2/s]
Weak, $W/C = 0.42$	60
Medium, W/C = 0.52	130
High, W/C = 0.73	200

The monolayer capacity is the adsorbed mass required to form a single layer of water vapour molecules on the cover concrete Eq. (13). The parameter k takes into account the fact that there could be several layers of molecules. Initially, Eq. (14) determines the number of layers n in the saturation state [57].

$$V_m = V_t(t) \cdot V_{WC}(W/C) \cdot V_{ct}(c_t) \cdot V_T(T) \quad (13)$$

$$n = N_t(t) \cdot N_{WC}(W/C) \cdot N_{ct}(c_t) \cdot N_T(T) \quad (14)$$

with:

t concrete curing time [days],
V_t (t) concrete curing time parameter,
V_{WC} (W/C) concrete composition parameter,
V_{Ct} (Ct) cement type parameter,
V_T (T) temperature effect parameter (The temperature effect is negligible compared to the C_{BET} parameter and is thus one),
n number of layers in the saturated state,
N_t (t) concrete curing time parameter,
N_{WC} (W/C) concrete composition parameter,
N_{Ct} (Ct) cement type parameter,
N_T (T) temperature effect parameter (The temperature effect is negligible compared to the C_{BET} parameter and is thus one.)

The effect of curing time is formulated by an empirical relation deduced from experimental results by [57]. When the curing time is below or equal to 5 days, its value is considered as constant Eqs. (17) and (18). If the curing time is above 5 days, it takes the form according to Eqs. (15) and (16):

$$V_t(t) = 0.068 - 0.22/t \quad N_t(t) = 2.5 - 15/t \quad \text{if } t > 5 \quad (15)(16)$$

$$V_t(t) = 0.068 - 0.22/5 = 0.024 \quad N_t(t) = 2.5 - 15/5 = 5.5 \quad \text{if } t \le 5 \quad (17)(18)$$

The effect of concrete composition is taken into account by the mass ratio of water to cement according to Eqs. (19) and (20) [57]:

$$V_{WC}(W/C) = 0.85 + 0.45 \cdot (W/C) \quad N_{WC}(W/C) = 0.33 + 2.2 \cdot (W/C) \quad (19)(20)$$

The type of cement is taken into account by constant values (Table 4) [57].

Finally, the parameter k is determined by Eq. (21) [57]:

$$k = \frac{\left(1 - \frac{1}{n}\right) \cdot C_{BET} - 1}{C_{BET} - 1} \quad (21)$$

The water content of the cement paste considers the water and cement amount present in the concrete composition, and a correction accounts for the water saturation in the concrete following Eq. (22):

$$w = \frac{w_c(H) \cdot (CP + CP \cdot E/CP)}{w_c(1)} \cdot w_{sat} \quad (22)$$

Table 4
Parameter values V_{Ct} and N_{Ct} according to the cement type [57].

Cement type	Standard use	V_{Ct}	N_{Ct}
Type I Portland cement	General use	0.9	1.1
Type II Portland composite cement	Hydration heat and moderate sulphate resistance	1	1
Type III blast furnace slag cement	High initial resistance at early concrete age	0.85	1.15
Type IV pozzolanic cement	Low hydration heat	0.6	1.5

with:

w_{sat} water content in the saturated state with respect to the concrete volume [kg/m^3].

The temperature effect on the adsorption isotherms remains small. The mass ratio W/C of water to cement represents the principal variability in this model.

The desorption curve modelling is carried out with Roelfstra's desorption model [43] as obtained from experimental results from samples of W/C ratios of 0.4, 0.45, 0.5 and 0.55, and at various temperatures ranging from 20 °C, 45 °C, 57 °C to 70 °C, Eqs. (23), (24), (25) and (26) [43].

$$\frac{w_r(H)}{\mathrm{CP}} = \frac{1}{(1-h_t)^2} \times \left(\begin{bmatrix} h_t^2 & 1-2\cdot h_t & h_t^2-h_t \\ -2\cdot h_t & 2\cdot h_t & 1-h_t^2 \\ 1 & -1 & h_t-1 \end{bmatrix} \cdot \begin{Bmatrix} E/\mathrm{CP}-c_4\cdot\alpha \\ \left(c_1+c_2\cdot h_t+c_3\cdot h_t^2\right)\cdot\alpha \\ (c_2+2\cdot c_3\cdot h_t)\cdot\alpha \end{Bmatrix} \right)^T \times \begin{Bmatrix} 1 \\ h \\ h^2 \end{Bmatrix} \quad \text{if } h_t \le h < 1 \tag{23}$$

$$\frac{w_r(H)}{\mathrm{CP}} = \left(c_1 + c_2\cdot h + c_3\cdot h^2\right)\cdot\alpha \quad \text{if } 0.35 \le h < ht \tag{24}$$

$$\frac{w_r(H)}{\mathrm{CP}} = \left[(-400\cdot c_1/49 + c_3)\cdot h + 40\cdot c_1/7 + c_2\right]\cdot\alpha\cdot h \quad \text{if } h < 0.35 \tag{25}$$

$$h_t = 1 - 0.161\cdot\alpha \tag{26}$$

with:

c_1, c_2 and c_3 material parameters according to Roelfstra's desorption model,

h_t limit of relative humidity when the model passes from a polynomial of second degree to another polynomial degree.

The material parameters c_1, c_2 and c_3 ensure desorption curve continuity at the relative humidity limit point Eqs. (23)–(26) [43].

The experimental test data and the results of the present model show a very good correlation [8]. Eq. (27) is a correction term considering the water content with concrete saturation:

$$w = \frac{w_r(H)}{w_r(1)}\cdot w_{sat} \tag{27}$$

Sudden changes in water content in the concrete can occur between two time intervals in the TransChlor simulations. Such cases frequently do appear when temperature variations are large or when concrete pore desorption or adsorption completely change with the most significant problems appearing in the cover concrete at the air–concrete interface. To advert these variations, a softer transition is modeled when the third nodes near the air–concrete interface exhibit a change greater than 5 [kg/m^3] over one hour time intervals. Eq. (28) is applied in this case and softens the water content evolution in time. This maximum change was defined by assessing the maximum possible variations and by using adsorption and desorption models identical to the isothermal state:

$$w_{t,\mathrm{final}} = w_{t-1} + \frac{w_t - w_{t-1}}{\Delta t/36} \tag{28}$$

with:

$w_{t,\mathrm{final}}$ water content with respect to the concrete volume in the transition zone between t and $t-1$ [kg/m^3],

w_{t-1} simulated water content with respect to the concrete volume at time $t-1$ [kg/m^3],

w_t simulated water content with respect to the concrete volume at time t [kg/m^3],

Δt time interval [s].

3.5. Hydrous transport of liquid water by capillary suction

Although Fick's law represents the effect of the water vapor diffusion rather well, it does not represent capillary suction values from experiments by [8,25]. Thus a new model is proposed for modeling water transport by capillary suction with kinetic equations. This proposed model closely simulates the documented capillary suction values. The capillarity coefficient was obtained directly from experimental results and is given in [8,9]. These results show that the capillarity coefficient depends on temperature. The parameters a_1, a_2 and a_3 are determined with Eq. (29):

$$\begin{Bmatrix} a_1 \\ a_2 \\ a_3 \end{Bmatrix} = \begin{bmatrix} 2.788\cdot10^{-7} & -7.355\cdot10^{-6} & -2.781\cdot10^{-4} & -1.231\cdot10^{-2} \\ -3.04\cdot10^{-7} & 7.975\cdot10^{-6} & 3.368\cdot10^{-4} & 1.779\cdot10^{-2} \\ 8.002\cdot10^{-8} & -2.262\cdot10^{-6} & -8.978\cdot10^{-5} & -4.608\cdot10^{-3} \end{bmatrix} \times \begin{Bmatrix} T^3 \\ T^2 \\ T \\ 1 \end{Bmatrix} \tag{29}$$

with a_1, a_2 and a_3 = parameters for computing the capillarity coefficient [−].

Additionally, the concrete composition and the concrete pore relative humidity are considered with Eq. (30):

$$D_{\mathrm{cap,to}} = \{\,100\cdot H \quad 1\,\} \cdot \begin{bmatrix} 6.248\cdot10^{-5} & -1.038\cdot10^{-4} & 3.003\cdot10^{-5} \\ a_1 & a_2 & a_3 \end{bmatrix} \times \begin{Bmatrix} (W/C)^2 \\ W/C \\ 1 \end{Bmatrix} \tag{30}$$

$D_{\mathrm{cap,to}}$ capillarity coefficient at liquid water contact [mm/s].

When capillary suction is initiated, the capillarity coefficient decreases as a function of time following Eq. (31). This reduction is due to the hydraulic pressure loss as the water front penetration increases.

$$D_{\mathrm{cap}} = D_{\mathrm{cap,to}}\cdot\left[\alpha_c + \frac{1-\alpha_c}{1+\left(\frac{1-t/10}{1-t_c}\right)^4}\right] \tag{31}$$

with α_c and t_c = capillarity model coefficients of 0.09 and 0.97 respectively, as obtained from experimental calibration.

In the TransChlor model, the capillarity coefficient in the first 40 mm of cover concrete is a function of the temperature and average relative moisture. The capillarity coefficient boundary conditions are assumed as shown in Fig. 1.

3.6. Chloride ions in concrete pores

The general formulation for chloride ion migration in the cover concrete considers the movement of aqueous chloride ions by diffusion and by water movement. By considering the total chloride ions

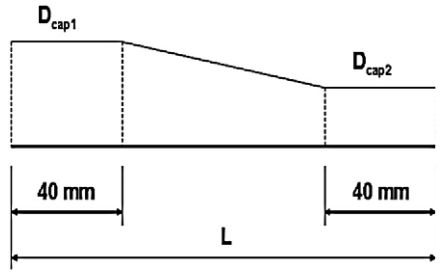

Fig. 1. Capillarity coefficient as a function of depth in the case of two activated boundary conditions.

as the sum of the free and bound chloride ions, the Freundlich's isotherm is inserted in Eq. (32):

$$C(B,T) = C_F + C_B = c_f \cdot w + c_f^{\beta} \cdot \gamma \tag{32}$$

with C_F concentration of free chloride ions in the concrete interstices per unit concrete volume [kg/m^3],
C_B concentration of chloride ions bound to the cement paste per unit concrete volume [kg/m^3],
w water content per unit concrete volume [m^3/m^3],
β Freundlich isotherm exponent (0.379),
γ Freundlich isotherm factor relating the total chloride ion concentration to the free chloride ion concentration.

The total chloride ion concentration is calculated at the end of each iteration by considering the local carbonation and temperature [24,42,52,53] leading to Eq. (33):

$$\gamma = e^{\alpha_{OH}\cdot\left(1-10^{pH-pHini}\right)} \cdot e^{\frac{Eb}{R}\left(\frac{1}{T}-\frac{1}{T0}\right)} \cdot \alpha \cdot CP \cdot 3.57 / 1000 \tag{33}$$

with:

α_{OH} model parameter, with a value of 0.56 [°C],
E_b activation energy in the Arrhenius' model [mol/J],
T_0 reference temperature in the Arrhenius' model [°C].

The diffusion of chloride ions in water [12] is modeled with Fick's law (1). The concrete mix characterized by the mass ratio of water and cement (Fig. 2) can be represented with the diffusion coefficient. In [8] the relationship between mass ratio of water and cement and the diffusion coefficient was deduced from a large number of experiments documented by [4,5,17,21,28–30,33,39,53]. The results of this study

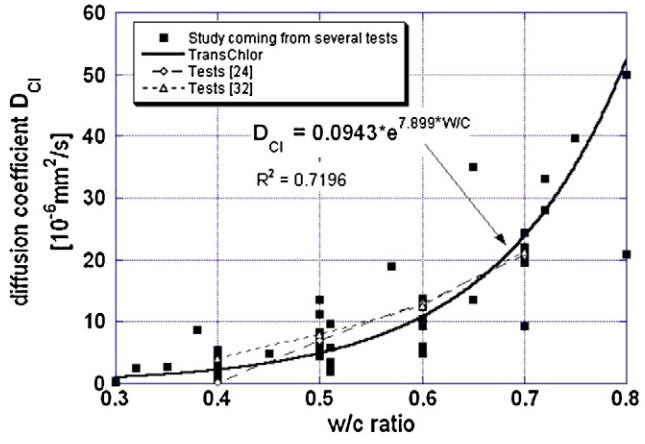

Fig. 2. Literature results for chloride ion diffusion coefficient as a function of W/C ratio under marine environment exposure.

have been compared with test results (Fig. 2) by [26,34] and it is observed that the diffusion coefficient is a function of the concrete composition (Fig. 2) and the temperature according to Arrhenius' law [56] (Eq. (34)):.

$$D_{Cl} = 0.0943 \cdot e^{7.899 \cdot W/C} \cdot e^{\alpha \cdot (T - T_0)} \tag{34}$$

W/C mass ratio of water and cement [−],
α model activation energy, with a value of 0.026 [°C^{-1}],
T_0 Arrhenius' model reference temperature, with a value of 20 °C [°C].

The chloride ion convection by water is controlled by water vapor and liquid water movement. The chloride ion convection in capillary liquid water suction is the fastest process for propagating the chloride ion front in the cover concrete [35,49]. Water vapor movement and the chloride ion convection are respectively modeled with Fick's diffusion equation and with the kinetics Eq. (1).

The chloride ion front exhibits a time delay as compared to the water front propagation. The delay coefficient, R_{Cl}, with a value ranging from 0.3 to 0.7 Eqs. (3) and (4) is thus introduced [25]. The specific value of this delay coefficient is still not accurately documented and, in the absence of additional results, a constant value for this coefficient is uniformly applied to chloride ion convection by liquid water and water vapor.

The equation for chloride ion convection by water is resolved by considering the water velocity at each node. Furthermore, the chloride ion concentration at each node undergoes a translation with respect to the water velocity and the delay coefficient R_{Cl} [44]. Unfortunately, when the translation is not uniform over all nodes, the conservation balance is no longer respected. To solve this problem, a different resolution step is proposed with an original algorithm [10].

4. Predictions and experimental results

The TransChlor model has been validated with experimental results from recent laboratory tests and findings documented in literature. Temperature, water absorption and chloride convection (in the specific case chloride pulled in by liquid water) were determined experimentally by different tests with moisture transport and carbonation results obtained from [36,57] respectively. Validation of the moisture transport model is presented in [57], and will not be further developed within this work. Finally, the aqueous chloride ion diffusion data in concrete pores is the result of extensive literature study of chloride diffusion coefficients (see Section 3 "Analytical Investigation" and Fig. 2).

4.1. Thermal diffusion process

The thermal diffusion was measured by documenting the results of several cubic samples exposed to an initial ambient temperature of 20 °C and then a constant reduced temperature of 10 °C, 0 °C, −10 °C and −20 °C. The thermal diffusion was particularly studied by exposing only one face of each cube to the reduced temperature (Fig. 3).

The laboratory measurements documented an identical thermal transfer rate for all the concrete specimens regardless their permeability or water content. TransChlor simulations do not exhibit the same tendency for the concrete permeability nor does water content influence the thermal transfer velocity. While the material variability can be important, the thermal transfer does not appear to change across different concretes or water content (Fig. 3). The water content evolution does not affect significantly thermal transfer during, for example, a drying–wetting process. Thus, the concrete thermal transfer velocity depends primarily on the concrete skeleton characteristics created by the cement paste and aggregates.

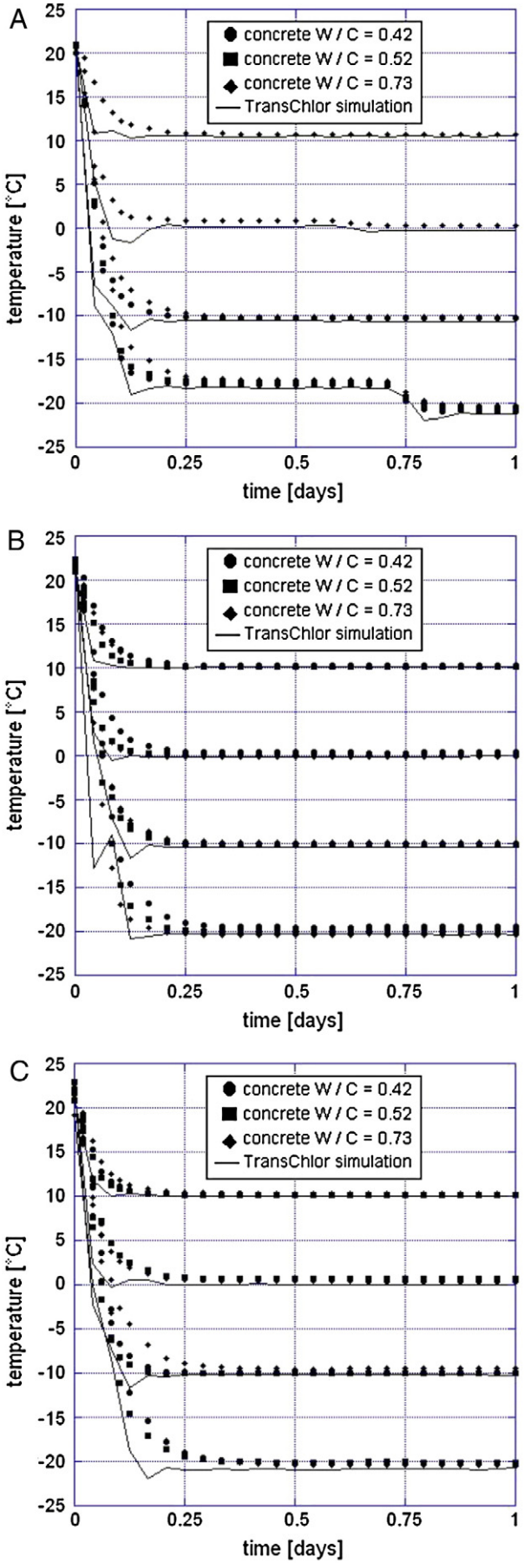

Fig. 3. TransChlor simulations of thermal diffusion in concrete and comparison with experimental results for relative humidity of: A) 75%, B) 50% and C) 25%.

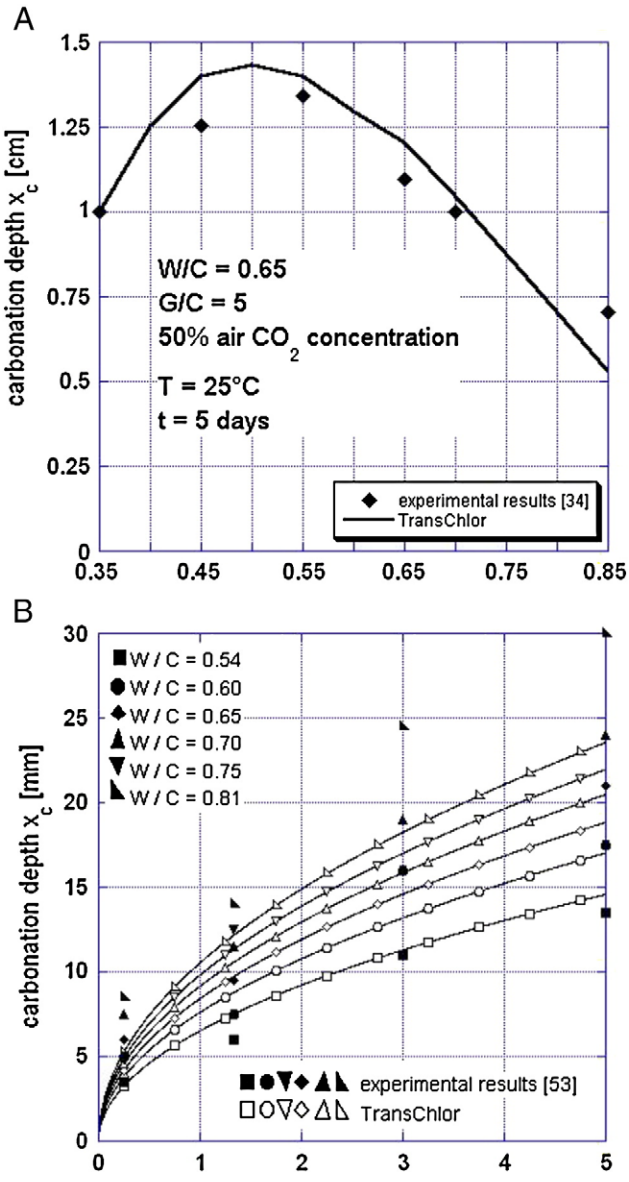

Fig. 4. TransChlor model simulations of carbonation depth and comparison with experimental results: effect of A) relative humidity, and B) concrete type (permeability).

The thermal variation in the cover concrete is a function of the external temperature variation. For the cover concrete, with a depth ranging from 25 to 30 mm, equilibrium between the internal and external temperatures was reached after 4 to 5 h. Thus the assumption employed by many researchers, to use the environmental atmosphere temperature as the internal temperature is sufficient given the time discretization used in the analytical model. The comparison between the laboratory measurements and the TransChlor simulations highlighted that the thermal transfer velocity is slightly more important for the model than for the experimental tests (Fig. 3).

4.2. Carbonation

The carbonation depths have been measured by [36] after 5 days of accelerated carbonation on concrete samples having a water to

cement ratio of 0.65 and a mass ratio of aggregates to cement of 5. The carbonation rate has been accelerated by increasing the carbon dioxide content in the air by 50% but the ambient temperature was maintained at 25 °C [36]. The carbonation rate was simulated on different relative air humidities and shows the carbonation rate increased for the concrete specimens stored at a relative humidity of 50%. The experimental results confirm this finding (Fig. 4A). These results highlight the influence of ambient conditions and, in particular the relative air humidity and the concrete water content have on the carbonation rate.

The concrete mix influence has been documented by carbonation tests conducted on concrete specimens with a cement content of 350 [kg/m^3] [55]. These carbonation tests were also accelerated by increasing the ambient carbon dioxide concentration to 20%. The tests documented that the concrete carbonation rate increases as the water to cement ratio increases. The TransChlor model simulates well the carbonation rate for low *W/C* ratio. The variability is more significant for specimens with a higher *W/C* ratio (Fig. 4B). An identical deviation was earlier identified with the air permeability tests conducted with the Torrent method [8,13].

4.3. Liquid water transport by capillary suction

A comparison with the test results of [25] was conducted by varying the characteristic parameters α_c and t_c. The total water adsorbed and the water content space profiles were measures for a set of specimens of various concrete mixes (Fig. 5A) and a *W/C* ratio of 0.5 at 6, 72 and 240 h (Fig. 5B). The parameters αc and tc corresponding to water adsorption (Fig. 5A) were 0.09 and 0.95 respectively and for the water content space profile (Fig. 5B) 0.05 and 0.97 respectively. Prior to the capillarity tests the samples were cured during at least two weeks in relative air humidity of 60% and at a temperature of 20 °C. Stable hydrous level due to drying was quickly reached after two weeks because of the small sample dimensions (thickness of about 1 cm).

4.4. Chloride ion concentration in the concrete pores

To validate TransChlor regarding chloride ion transport, experimental results for capillarity tests have been carried out on a specimen made of concrete with *W/C* ratio of 0.52 (average permeability). This specimen was equipped with a newly developed optical fiber sensor for chloride detection [22]. This sensor is a chemical detector using optical fibers exploiting the sensitive fluorescence intensity attenuation principle of a chloride ion indicator. By means of the fluorescence spectroscopy analysis that is often used in biochemistry and medical domain, free chloride ion concentrations in the pore water of concrete has been determined. This small size sensor that is easy to position in various depths in the cover concrete is insensitive to magnetic fields. Moreover, it offers the advantages of non-destructive measurement methods.

After 31 days of curing, the specimen was immersed in a 3% brine solution. The sensor position was at 18 mm from the concrete surface (Fig. 6A). Measurements and TransChlor results present good correspondence after 8 days which confirm correct model response for long-term values (Fig. 6B). In the shorter term, the increase in free chloride ion concentration is qualitatively similar between experimental and simulation results.

The model and measurements highlight well the propagation of the chloride ion front which is characterized by a fast increase of the

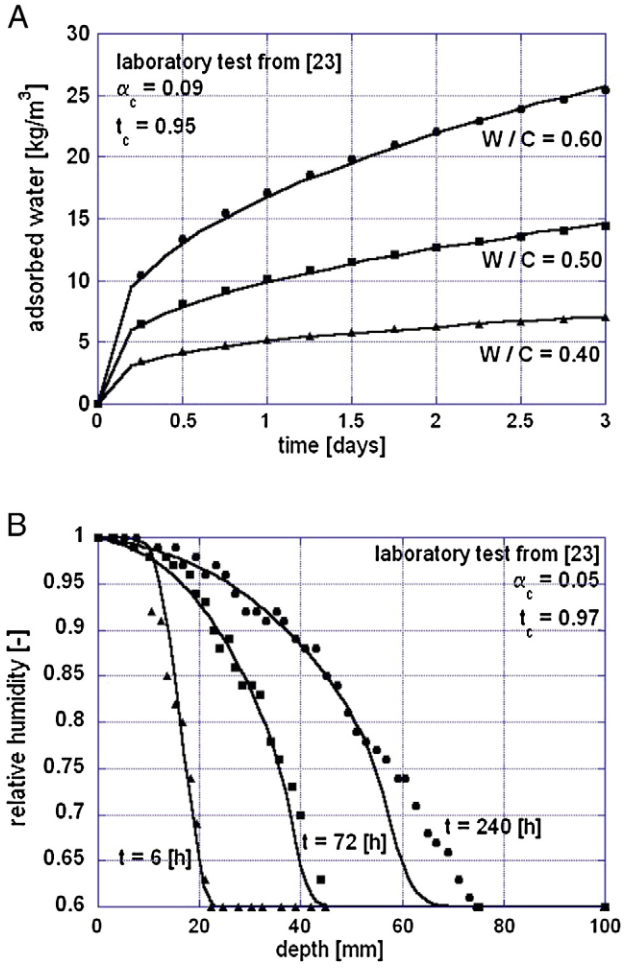

Fig. 5. Comparison of capillarity tests by [25] with the TransChlor simulations: A) evolution and B) profiles of adsorbed water in concrete.

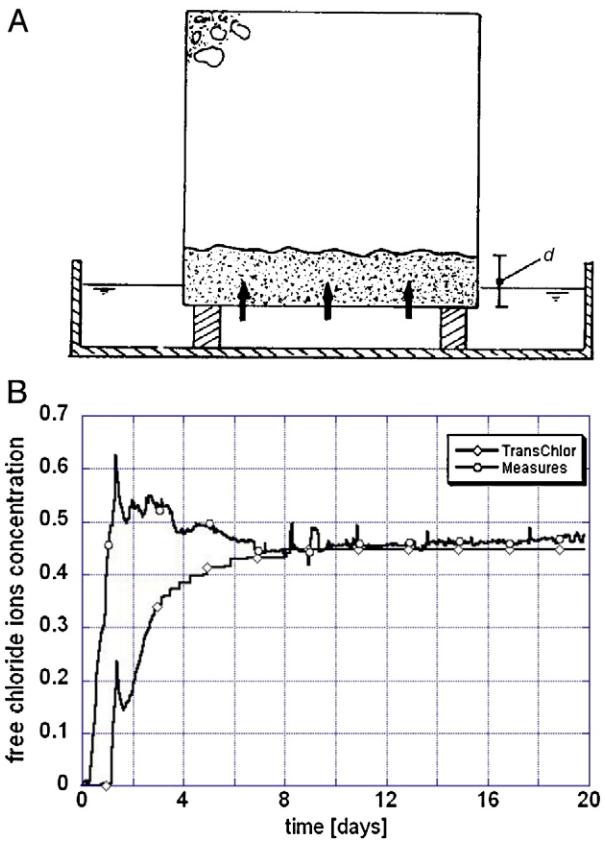

Fig. 6. Capillarity test on a cubic specimen equipped with a chloride ion sensor [22], A) test set-up, and B) comparison of TransChlor simulation and experimental results.

chloride ion concentration at 18 mm depth from the concrete surface already after several days of brine exposure.

5. Conclusions

1. TransChlor is a numerical model based on the finite element and finite difference methods. This comprehensive model combines various transport modes, i.e. thermal transfer, hydrous transfer of vapor water and liquid water by capillary suction, carbon dioxide diffusion, chloride ion diffusion and chloride ion convection by the hydrous movement.
2. TransChlor is made for including real climate. Transchlor converges when sudden changes appear in the boundary condition, for example if a rain period succeeds at a dry period.
3. Liquid water movement by capillary suction is modeled by the kinematic equations. These equations are transformed to obtain chloride ion movement, simulating in this way chloride ion convection by water using a particular algorithm. This novel approach is validated by experimental results.
4. TransChlor model simulations and optical fiber sensors show that the chloride ion front traverses 18 mm of cover concrete within a few days when a dry concrete sample is in contact with water. This finding opens the way to the combined analysis by experimental results obtained by a newly developed chloride ion sensor with optical fibers and sophisticate numerical model.

References

[1] V. Baroghel-Bouny, 1994, Caractérisation des pâtes de ciment et des bétons, LCPC et ministère de l'équipement des transports et du tourisme, 468, Paris, France.
[2] Z. Bazant, L.J. Najjar, Drying of concrete as a nonlinear diffusion problem, Cement and Concrete Research, vol. 1, 1971, pp. 461–473, USA.
[3] Z. Bazant, August 1986, Creep and Shrinkage of Concrete: Mathematical Modeling, RILEM, 10, Illinois, United States.
[4] D.P. Bentz, Influence of silica fume on diffusivity in cement-based materials. II Multi-scale modeling of concrete diffusivity, Cement and Concrete Research, vol. 30, Pergamon, Gaithersburg, U.S.A., 2000, pp. 1121–1129.
[5] T. Callanan, M. Richardson, 2003, Modelling Chloride Ingress in Concrete: A Comparative Study of Laboratory and Field Experience, Sixth Canmet/ACI International Conference, 1, 389 – 408, Thessaloniki, Greece.
[6] T. Chaussadent, Etat des lieux et réflexions sur la carbonatation du béton armé, LCPC, Paris, France, Septembre 1999.
[7] D. Conciatori, E. Denarié, H. Sadouki, E. Brühwiler, Chloride penetration model considering the microclimate, The 3rd International IABMAS Workshop, Lausanne, Switzerland, March 2003, pp. 24–26.
[8] D. Conciatori, Effet du microclimat sur l'initiation de la corrosion des aciers d'armature dans les ouvrages en béton armé, thèse n° 3408, Ecole Polytechnique Fédérale de Lausanne, Lausanne, 2005.
[9] D. Conciatori, E. Brühwiler, Sub-zero transport: low temperature capillary tests in concrete, in: J. Marchand, R. Gagné (Eds.), 2nd International RILEM Symposium, Advances in Concrete through Science and Engineering, cds publication, Quebec City, Canada, 2006, Publisher Information.
[10] D. Conciatori, H. Sadouki, E. Brühwiler, Capillary suction and diffusion model for chloride ingress into concrete, Cement and Concrete Research 38 (2008) 1401–1408.
[11] D. Conciatori, E. Brühwiler, A.G. Dumont, Actions climatique et environnementale des ouvrages d'art routier, Canadian Journal of Civil Engineering 36 (4) (2009) 628–638.
[12] A. Delagrave, J. Marchand, E. Samson, Prediction of diffusion coefficients in cement-based materials on the basis of migration experiments, Cement and Concrete Research, 26 (1996) 1831–1842.
[13] E. Denarié, M. Maître, D. Conciatori, E. Brühwiler, Air permeability measurements for the assessment of the in situ permeability of cover concrete, International Conference on Concrete Repair, Rehabilitation and Retrofitting, Cape Town, South Africa, November 2005.
[14] I. Denisov, Décembre 2004, Etude de l'hydratation et du couplage carbonatation-échanges hydriques dans les mortiers et bétons, Université de la Rochelle - UFR Sciences, Rochelle, France.
[15] R.K. Dhir, E.A. Byars, PFA Concrete: Chloride diffusion rates, Magazine of Concrete Research 45 (1993) 1–9.
[16] R. Drochytka, V. Petranek, 2001, Atmospheric Concrete Deterioration, FIB, Proceedings of the First Fib Congress, pp 189–198, Brno, Czech Republic.
[17] P. Halamickova, R.J. Detwiler, Water permeability and chloride ion diffusion in Portland cement mortars: relationship to sand content and critical pore diameter, Cement and Concrete Research 25 (1995) 790–802.
[18] H. Hamfler, 1988, Berechnung von Temperatur -, Feuchte- und Verschiebungsfeldern in erhärtenden Betonbauteilen nach der Methode der finiten Elemente, Deutscher Ausschuss für Stahlbeton, Heft 395, 159 p., Berlin, Germany.
[19] T. Ishida, K. Maekawa, 2000, A Computational Method for Performance Evaluation of Cementitious Materials and Structures under Various Environmental Actions, 5 p., Tokyo, Japan.
[20] M. Janz, 1997, Methods of Measuring the Moisture Diffusivity at High Moisture Levels, Thesis, University of Lund — Division of Building Materials, 73, Lund, Sweden.
[21] T.J. Kirkpatrick, R.E. Weyers, M.M. Sprinkel, C.M. Anderson-Cook, 2002, Impact of Specification Changes on Chloride-Induced Corrosion Service Life of Bridge Decks, Cement and Concrete Research, Pergamon, 32, 1189–1197, Blacksburg, U.S.A.
[22] F. Laferrière, 2005, Surveillance des ouvrages de génie civil par capteurs à fibres optiques: capteurs d'ions chlore, Ecole Polytechnique Fédérale de Lausanne, Thèse n° 3322, 159 p., Lausanne, Suisse.
[23] F. Larrard, T. Sedran, D. Kaplan, 1999, Rhéologie des bétons fluides, Monographie d'études et de recherches 1996–1997, Réseau des LPC.
[24] A. Lindvall, 2001, Environmental actions and response, reinforced concrete structures exposed in road and marine environments, Chalmers University of technology, P-01:3, 320 p., Göteborg, Sweden.
[25] P. Lunk, 1998, Penetration of Water and Salt Solutions Into Concrete by Capillary Suction, Internationale Zeitschrift für bauinstandsetzen, 4, 399–422, Zürich, Suisse.
[26] K.A. MacDonald, D.O. Northwood, Experimental measurements of chlorid'ion diffusion rates using a two-compartment diffusion cell: effect of material and test variables, Cement and Concrete Research 25 (1995) 1407–1416.
[27] K. Maekawa, T. Ishida, Service-Life Evaluation of Reinforced Concrete under Coupled Forces and Environmental Actions, University of Tokyo, Tokyo, Japan, 2000 20 pp.
[28] J. Marchand, 2001, Modeling the Behavior of Unsatured Cement Systems Exposed to Aggressive Chemical Environments, Materials And Structures, 34, Quebec, Canada.
[29] J. Marchand, E. Samson, Y. Maltais, R.J. Lee, S. Sahu, December 2002, Predicting the Performance of Concrete Structures Exposed to Chemically Aggressive Environment-Field Validation, Materials and Structures, 35, pp 623 – 631, Quebec, Canada.
[30] J. Marchand, E. Samson, Y. Maltais, R.J. Lee, 2002, Predicting the Performance of Concrete Structures Exposed to Chemically Aggressive Environments-Fields Validation, 2nd Material Specialty Conference of the Canadian Society for Civil Engineering, 1–13, Quebec, Canada.
[31] M. Masi, D. Colella, G. Radaelli, L. Bertolini, 1997, Simulation of Chloride Penetration in Cement-Based Materials, Cement and Concrete Research, Pergamon, Elsevier Science Ltd., 27, No. 10, 1591–1601, Milan, Italy.
[32] S.J.H. Meijers, 2003, Computational Modeling of Chloride Ingress in Concrete, DUP science, Delft University Press, 170, Delft, Holland.
[33] W. Morris, M. Vasquez, August 2001, A Migrating Corrosion Inhibitor Evaluated in Concrete Containing Various Contents of Admixed Chlorides, Cement and Concrete Research, 32, 259–267, U.K.
[34] V.T. Ngala, C.L. Page, L.J. Parrott, S.W. Yu, Diffusion in cementitious materials: II Further investigations of chloride and oxygen diffusion in well-cured OPC and OPC/30% PFA pastes, Cement and Concrete Research 25 (1995) 819–826.
[35] L.-O. Nilsson, E. Poulsen, U. Sandberg, M.G. Sorensen, O. Klinghoffer, 1996, HETEK, Chloride Penetration into Concrete, State-of-Art, Transport Processes, Corrosion Initiation, Test Methods and Prediction Models, The Road Directorate, Report n° 53, 150 p., Copenhagen, Scandinavia.
[36] V.G. Papadakis, M.N. Fardis, C.G. Vayenas, 1990, Fundamental Concrete Carbonation Model and Application to Durability of Reinforced Concrete, Fifth International Conference Durability of Building Materials and Components, Proceedings, pp 27–38, Brighton, England.
[37] V.G. Papadakis, C.G. Vayenas, M.N. Fardis, March–April 1991, Physical and Chemical Characteristics Affecting the Durability of Concrete, ACI Materials Journal, V. 8, No 2, pp 186 – 196, Copenhagen, Denmark.
[38] V.G. Papadakis, February 2000, Effect of Supplementary Cementing Materials on Concrete Resistance Against Carbonation and Chloride Ingress, Cement and Concrete Research, Volume 30, Issue 2, pp 291–299, Taastrup, Denmark.
[39] B. Persson, March 2004, Chloride Migration Coefficient of Self-Compacting Concrete, Materials and Structures RILEM Publications, vol. 37, 82–91, Lund, Sweden.
[40] K.H. Pettersson, May 1996, Factors Influencing Chloride-Induced Corrosion of Reinforcement in Concrete, 7, 334 – 341, Gälve, Sweden.
[41] M. Richardson, 2002, Fundamentals of Durable Reinforced Concrete, Modern Concrete Technology, 11, 259 p., New York, United States of America.
[42] W. Ritthichauy, T. Sugiyama, Y. Tsuji, T. Suda, 2001, Thermodynamic Law Applied for the Diffusion of Chlorid'ions Ion Concrete, FIB, Proceedings of the 1st fib Congress, pp 115 – 120, Gunma, Japan.
[43] P.E. Roelfstra, 1989, A Numerical Approach to Investigate the Properties of Concrete — Numerical Concrete, EPFL, Swiss Federal Institute of Technology, Doctoral Thesis, N° 788, Lausanne, Switzerland.
[44] G. Roelfstra, 2000, Modèle d'évolution de l'état des ponts-routes en béton, Thèse de doctorat, Ecole Polytechnique Fédérale de Lausanne, Thèse N° 2310, 153, Suisse.
[45] A.V. Saetta, R.V. Scotta, R.V. Vitaliani, Analysis of chloride diffusion into partially saturated concrete, ACI Materials Journal 90 (5) (1993) 441–451.
[46] A.V. Saetta, B.A. Schrefler, R.V. Vitaliani, 2-D model for carbonation and moisture/heat flow in porous materials, Cement and Concrete Research 25 (1995) 1703–1712.
[47] A.V. Saetta, R.V. Vitaliani, September 2003, Experimental Investigation and Numerical Modeling of Carbonation Process in Reinforced Concrete Structures Part I: Theoretical Formulation, Cement and Concrete Research, 9 p., Padova, Italy.
[48] E. Samson, J. Marchand, K.A. Snyder, J.J. Beaudoin, June 2004, Modeling Ion and Fluid Transport in Unsaturated Cement Systems for Isothermal Conditions, 31 p., Quebec, Canada.
[49] Y. Schiegg, H. Böhni, F. Hunkeler, 2002, Online-Monitoring of Corrosion in Reinforced Concrete Structures, FIB, Proceedings of the 1st Fib Congress, pp 49–58, Zurich, Switzerland.
[50] F. Schmidt-Döhl, F.S. Rostasy, 1999, A Model for the Calculation of Combined Chemical Reactions and Transport Processes and Its Application to the Corrosion

of Mineral-Building Materials Part I. Simulation Model, Elsevier Science Ltd., Part I Simulation model, pp 1039–1045, Braunschweig, Germany.
[51] C.B. Shin, E.K. Kim, December 2001, Modeling of Chlorid'ion Ingress in Coastal Concrete, A. A. Balkema, 32, 757–762, South Korea.
[52] T. Sugiyama, W. Ritthichauy, Y. Tsuji, Simultaneous transport of chloride and calcium ions in hydrated cement systems, Journal of Advanced Concrete Technology 1 (2) (July 2003) 127–138.
[53] L. Tang, 1996, Chloride Transport in Concrete — Measurements and Prediction, Chalmers University, P-96:6 Abr. Nr. 546, Göteborg, Sweden.
[54] O. Truc, J.P. Ollivier, O. Nilsson, September 2000, Multi Species Transport in Saturated Cement-Based Materials, RILEM, proceeding PRO 19, edited by C. Andrade and J. Kropp, Pro 19, 14, Toulouse, France.
[55] M. Vénuat, J. Alexandre, 1969, De la carbonatation du béton, Revue des matériaux de construction, 638, 1–50, Paris, France.
[56] T. Zhang, E. Samson, J. Marchand, 2005, Effect of Temperature on Ionic Transport Properties of concrete, Simco Technologies Inc, Quebec, 11 p., Quebec, Canada.
[57] Y. Xi, Z. Bazant, H.M. Jennings, 1994, Moisture Diffusion in Cementitious Materials — Adsorption Isotherms, Advanced Cement Based Materials, Vol. 1, pp 248–257, USA.